ACS SENSORS

pubs.acs.org/acssensors

Article

# Passive and Flexible Wireless Electronics Fabricated on Parylene/PDMS Substrate for Stimulation of Human Stem Cell-Derived Cardiomyocytes

Ahmed Abed Benbuk,[‡] Hamid Esmaeili,[‡] Shiyi Liu, Alejandra Patino-Guerrero, Raymond Q. Migrino, Junseok Chae, Mehdi Nikkhah,* and Jennifer Blain Christen*

Cite This: *ACS Sens.* 2022, 7, 3287−3297

Read Online

ACCESS | Metrics & More | Article Recommendations | Supporting Information

**ABSTRACT:** In this paper, we report the development of a wireless, passive, biocompatible, and flexible system for stimulation of human induced pluripotent stem cell derived cardiomyocytes (hiPSC-CMS). Fabricated on a transparent parylene/PDMS substrate, the proposed stimulator enables real-time excitation and characterization of hiPSC-CMs cultured on-board. The device comprises a rectenna operating at 2.35 GHz which receives radio frequency (RF) energy from an external transmitter and converts it into DC voltage to deliver monophasic stimulation. The operation of the stimulator was primarily verified by delivering monophasic voltage pulses through gold electrodes to hiPSC-CMs cultured on the Matrigel-coated substrates. Stimulated hiPSC-CMs beat in accordance with the monophasic pulses when delivered at 0.5, 1, and 2 Hz pulsing frequency, while no significant cell death was observed. The wireless stimulator could generate monophasic pulses with an amplitude of 8 V at a distance of 15 mm. These results demonstrated the proposed wireless stimulator's efficacy for providing electrical stimulation to engineered cardiac tissues. The proposed stimulator will have a wide application in tissue engineering where a fully wireless stimulation of electroconductive cells is needed. The device also has potential to be employed as a cardiac stimulator by delivering external stimulation and regulating the contractions of cardiac tissue.

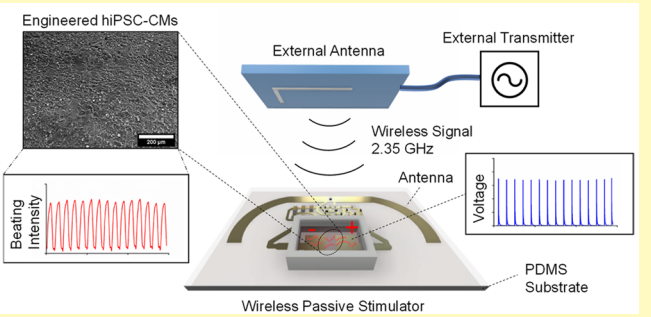


**KEYWORDS:** *Wireless stimulator, Passive biocompatible rectenna, RF energy harvesting, Stem cells, hiPSC-CMs, Cardiac tissue*

Cardiac pacing technology has advanced tremendously since the implantation of the earliest pacemaker back in the 1950s.[1] In a cardiac pacemaker, stimulation, electrical voltage pulses, can be delivered using an electrode pair that is placed in contact with the cardiac tissue. The pulse generator can be positioned subcutaneously via surgery with leads connecting the generator to the electrodes inserted into cardiac chambers through the subclavian vein.[2] However, lead failure has been reported as the underlying reason for the long-term complications, including bleeding and infection.[2,3] To avoid these complications, leadless pacemakers were developed in the 1970s.[4] In leadless pacemakers, the implanted signal generator and the electrodes are integrated in a compact form positioned directly contacting the target cardiac tissue. However, the currently approved leadless pacemakers still require using batteries, which limits their chronic applications. Additionally, recurring surgeries are required for battery replacement.[5,6]

Electrical stimulation has also been used for cardiac tissue maturation *in vitro*.[7−11] Electrical stimulation for enhanced maturation of engineered heart tissues was first performed by Radisic et al.[12] In that study, 8 days of electrical stimulation resulted in cell alignment and coupling along with ultrastructural organization in the engineered cardiac tissues derived from neonatal rat ventricular myocytes (NRVMs). Since then, multiple studies have reported the benefit of electrical pulse stimulation for the enhanced maturation of cardiac tissues derived from either NRVMs[7,8] or hiPSC-CMs.[8−10] However, in these studies, the electrical stimulation was performed through wired systems.

Passive wireless stimulators, which rely on harvesting RF energy, have been considered an effective solution to deliver stimulation while eliminating leads and batteries. Wireless stimulators are being developed for several applications including cardiac[13,14] and neural stimulation.[15−17] While both cardiac and neural stimulators have a similar general structure that includes a wireless element, rectifier, and electrodes, cardiac

**Received:** April 13, 2022
**Accepted:** September 29, 2022
**Published:** October 25, 2022

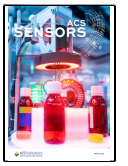

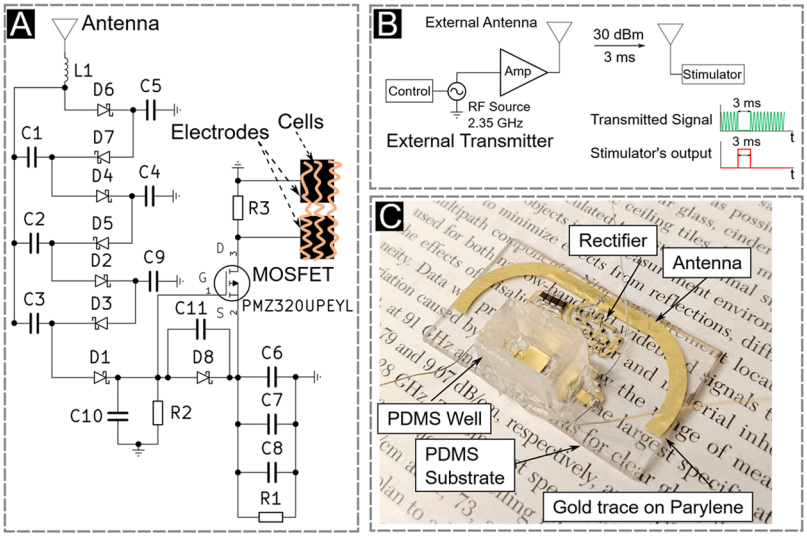


**Figure 1.** Proposed wireless and passive stimulator. (A) A schematic of the proposed wireless stimulator circuit with on-board culturing capability. (B) A system block diagram showing the stimulation setup. The external transmitter controls the stimulation frequency and the pulse width by generating a modulated signal, which is received and converted into monophasic pulses by the stimulator. (C) A fabricated wireless stimulator on parylene/PDMS substrate, highlighting the transparency of the device. A PDMS well with a height of 10 mm is incorporated for cell culturing. The wires connected on the device are only used for testing and measurement purpose.

stimulators are required to generate voltage and current with a higher amplitude to obtain a response. On the other hand, cardiac stimulators are less constrained in terms of size and channel number when compared with neural stimulators.

The wireless element can be either an antenna or a coil. An external coil can be used to supply energy to the stimulator which is equipped with a receiving coil and a rectifier to convert the signal into a DC voltage.[14−18] The two coils can be used to transfer RF energy with high efficiency at a few millimeters, and the output voltage depends on the size and distance between the two coils.[14] In a study by Choi et al.,[14] for example, a bioresorbable leadless and battery-free cardiac pacemaker was developed and tested in various animals *in vivo* including mouse, canine, and human cardiac models. A large external coil with a size of up to 260 × 280 $mm^2$ was required for powering the device.

As an alternative to coils, antennas can be used to deliver the energy from the transmitter to the stimulator. The advantage of antennas includes higher gain and reduced footprints as compared to coils.[19,20] For example, Liu et al. demonstrated the possibility of electrical stimulation of cardiac tissues derived from NRVMs through a wireless stimulator powered by an antenna operating at 2.4 GHz.[21] The stimulator contains gold electrodes fabricated on a polyimide substrate which were connected to carbon electrodes via platinum wires. When relying on antennas to harvest RF power, the size of the receiver's antenna can be reduced through meandering,[22] physical modification to prolong the surface current and return path,[23,24] or dielectric loading using a substrate with a high relative dielectric constant.[20,24] Biocompatibility of the stimulator is essential for implantable applications, and it is often realized using a biocompatible enclosure[25,26] or coating.[22,27] Polydimethylsiloxane (PDMS) has been recently investigated as a potential substrate material for wearable and implantable RF circuits.[28−31] PDMS has the advantages of biocompatibility, flexibility, transparency, and low cost. However, the main challenge when employing PDMS in high frequency applications is its low and unpredictable dielectric constant and high loss tangent. The low dielectric constant and high loss tangent complicate the design and miniaturization of the antenna and rectifier. Several studies have been conducted recently to determine the dielectric constant of PDMS.[32,33] For example, a dielectric constant of 2.76−3 based on two characterization methods at a frequency between 1 to 5 GHz, and a loss tangent of 0.01 is reported. Values within this range are commonly used in full electromagnetic simulation.[32] PDMS has been considered as a coating material for stimulator systems which operate at a low frequency wireless signal;[13,14,34,35] however, its potential as the main substrate for high frequency stimulators remains unexplored. In addition, there is a need to simplify the stimulator's circuit and introduce the ability to generate monophasic pulses with an amplitude of at least 2−3 V for cardiac stimulation without requiring complex hardware such as a microcontroller[15,25] or active components that demand constant biasing.[16] As for the external transmitter, it is crucial to maintain a small overall footprint to minimize the system's impact on mobility for *in vivo* applications.

This paper presents a wireless, passive, flexible, and biocompatible stimulator fabricated on a parylene/PDMS substrate (thickness = 0.6 mm). To verify its functionality and biocompatibility, we employ the wireless stimulator to stimulate cultured hiPSC-CMs. The gold conductive traces are sputtered on a thin sheet of parylene which exhibits a strong bond to the sputtered gold traces while maintaining flexibility and transparency. Thus far, *in vitro* electrical stimulation of cultured hiPSC-CMs has only been carried out by wired instrumentation.[8−10,36−38] To the best of our knowledge, this work is the first to implement an antenna and rectifier on a PDMS substrate for the *in vitro* stimulation and pacing of hiPSC-CM-derived cardiac tissues. In this work, the entire cell-culturing and stimulation processes were performed wirelessly on-board to prove the efficacy of the proposed wireless stimulator. Our results demonstrated that beating frequencies of the cultured hiPSC-CMs were regulated when wireless stimulation was delivered at various frequencies (0.5, 1, and 2 Hz). These stimulation frequencies were selected to test the wireless stimulator's ability


https://doi.org/10.1021/acssensors.2c00794
ACS Sens. 2022, 7, 3287−3297

to pace hiPSC-CMs because they are within the resting heart rate of a healthy adult human. These values are common in studies that involve stimulation and maturation of human derived cultured cardiac cells.[8−10] RF energy is harvested from a small external antenna with dimensions of $1 \times 1$ cm$^2$ at range up to 85 mm. The stimulator does not include any complex digital components, voltage regulators, or operational amplifiers that are widely used to boost the stimulator's DC output voltage and generate a monophasic stimulation signal.[15,16] Instead, the stimulator features a single MOSFET to deliver monophasic stimulation pulses to the cultured hiPSC-CMs with a maximum voltage of 8 V. Overall, this work demonstrates the realization of a wireless stimulator on a parylene/PDMS substrate, revealing the utility of this material combination to mechanically support the antenna and high frequency electronics, while maintaining a small thickness, transparency, and biocompatibility. By using a simple and effective circuit design, the stimulator generates monophasic pulses which successfully regulate the contraction of engineered cardiac cells. These results suggest the promising potentials of employing Parylene/PDMS as a transparent, flexible, and biocompatible substrate for RF implantable electronic applications.

## MATERIALS AND METHODS

**Passive Wireless Stimulator.** Cardiac stimulation can be performed by delivering monophasic pulses with a duration of a few milliseconds at a frequency of a few Hertz.[10,37] A voltage magnitude of at least a few volts is required to drive an electrical current in the cardiac tissue.[10,37] Figure 1A shows a circuit diagram of the proposed stimulator which employs RF coupling to convert the wireless signal into DC voltage. It comprises a printed meandered dipole antenna operating at the 2.35 GHz, followed by a Dickson voltage multiplier. We selected this antenna type because it has a simple structure and does not require a conductive ground plane that compromises the device's transparency. The antenna was simulated on a parylene/PDMS substrate with dielectric constant $\varepsilon_r = 3$. It was found that using this dielectric constant value yields measured results that closely resemble the simulated values. The impedance and radiation characteristics of the antenna are described in more detail in the Supporting Information (Figure S-1). The antenna is designed as a half-wavelength dipole on a PDMS substrate, and its length was tuned through parametric sweep simulation in Ansys Electronics software to optimize the performance at 2.35 GHz. Meandering of the antenna was performed through several iterations to obtain the finalized shape shown in Figure S-1A, leaving space in the center for placing electronics and the electrodes. A matching series inductor (Ceramic Chip inductor, 0.3 nH, Murata) was used to cancel the negative imaginary input impedance of the rectifier and maximize the power transfer between the antenna and the load. The rectifier was composed of several Schottky diodes (JDH2S02SL, Toshiba) that were connected in a Dickson voltage multiplier configuration to obtain the required output DC voltage that was accumulated in a 30 $\mu$F storage capacitor (C6−C8). An enhancement-type P-MOSFET (PMZ320UPEYL, Nexperia) was leveraged as a passive switch to deliver the harvested energy to the cultured human induced pluripotent stem cell-derived cardiomyocytes (hiPSC-CMs) in the form of electrical current. The operation of the P-MOSFET was controlled using a timing circuit (R2 and C10) that was connected to the gate. The timing circuit charges on the output of the voltage multiplier and reaches a steady state voltage that is equal to the harvested voltage across the storage capacitor, i.e., $V_{GS} \approx 0$ V. In this state, the switch was OFF, and no current was delivered to the cells. The P-MOSFET switch can be switched ON by discharging the voltage stored in the timing circuit.

**External Transmitter.** The external transmitter was composed of a frequency synthesizer (5009, Valon) and an amplifier (MPA-24−20, RF Bay, Inc.) to boost the transmitted signal power to 30 dBm. An external antenna (A10194, Antenova) was utilized at the transmitter. The external transmitter performs On−Off-keying (OOK) modulation and switches OFF the carrier signal for a period of 3 ms at a maximum frequency of 2 Hz to stimulate the cells as shown in Figure 1B. The timing circuit, characterized by a small time constant, discharges when the carrier signal is switched OFF, and the P-MOSFET switch turns ON ($V_{GS} < 0V$), which opens the drain−source channel. Therefore, current was delivered to the hiPSC-CMs by discharging the voltage accumulated on the storage capacitor. The proposed stimulator is passive because it does not require any biasing sources for harvesting, timing, or switching functions. In addition, the external transmitter can be operated without requiring complex modulation of the carrier. The frequency and width of the stimulation pulse was controlled by the external transmitter. The maximum transmit power at the output of the amplifier was set to 30 dBm, in line with Federal Communication Commission (FCC) regulations.[39]

**Passive Wireless Stimulator Fabrication.** The stimulator circuit was fabricated by depositing gold traces on a parylene layer that was attached to PDMS substrate, as shown in Figure 1C. We chose to sputter the gold traces on a thin parylene substrate on top of a thick PDMS substrate because parylene provides good bonding of the sputtered gold. However, parylene alone is not suitable to be the device substrate because it is not transparent at a thickness that provides good structural support for the device. Therefore, we adopt a the parylene/PDMS structure to provide structural support while maintaining transparency. The parylene and PDMS thicknesses are 20 $\mu$m and 0.6 mm, respectively. A detailed description of the fabrication steps is provided in the Supporting Information (Figure S-2). In addition, a prototype circuit fabricated on a Rogers 6010 substrate was used to compare the rectifier's output DC voltage for different number of multiplier stages (Figure S-3). The output DC voltage for an increasing number of Dickson multiplier stages is shown in Table S-I. The meandered dipole antenna was characterized by a length of 59.4 mm and width of 2.5 mm, and the rectifier circuit occupies an area of $6.9 \times 16.8$ mm$^2$. Figure 1C shows an image of a fabricated wireless stimulator. Note that the transparency of the PDMS substrate enables clear observation of the text below the device. In addition, a region with dimensions of $13 \times 9$ mm$^2$ is dedicated for cell culturing. It contains two gold electrodes, each having dimensions of $5 \times 3.5$ mm$^2$, and they are separated by 1.8 mm. A PDMS cell culture well with a volume of $6.9 \times 16.8 \times 10$ mm$^3$ was incorporated into the device to retain the cultured cells and media. The cell culturing well shown in Figure 1C is attached to the soft Parylene/PDMS substrate using transparent silicone adhesive. $O_2$ plasma treatment is not applied as it may damage the surface-mount electronics. The cell culturing well defines the surface area for contact with the cultured cardiac cells, and it is used as a vessel to hold the cells for the cell culture protocol. For future in vivo applications, the well will be eliminated.

**Differentiation of hiPSCs toward Ventricular Like Cardiomyocytes (CMs).** Human-induced pluripotent stem cells (hiPSCs; IMR90−4) were obtained from WiCell. The differentiation was based on the previous published method of modulation of Wnt/$\beta$-catenin signaling with slight modifications.[40−42] hiPSCs were maintained on Matrigel-coated plates in mTeSR1 medium that was changed every 24h. The hiPSCs were passaged at around 80% confluence. Monolayer differentiation of hiPSCs toward cardiac lineage was initiated at 85−95% confluence by substituting the mTeSR1 medium with RPMI + B27 minus insulin medium supplemented with 1% penicillin/streptomycin (PenStrep), which was designated as day 0 (D0). During the first 24 h, the medium was supplemented with 8 $\mu$M small molecule CHIR99021 (BioVision) that activates the Wnt pathway by inhibiting the Glycogen Synthase Kinase-3 (GSK) pathway. After 24 h of Wnt activation (D1), the medium was replaced by RPMI + B27 minus insulin, allowing cell recovery. On D3, the medium was replaced by a 1:1 rpmI + B27 minus insulin and the conditioned medium from the cell culture that was supplemented with 5 $\mu$M IWP-2 (Sigma). From D5 to D7, the cells were maintained in RPMI + B27 minus insulin for recovery. From D7 to D13, cells were maintained in RPMI + B27 to enhance cardiac maturation, and the medium was changed every 48 h. The characteristic spontaneous beating of the hiPSC-CMs was observed around days 9−12 of differentiation. From D13 to D19, the medium was replaced by


https://doi.org/10.1021/acssensors.2c00794
ACS Sens. 2022, 7, 3287−3297

glucose-free RPMI + B27 supplemented with 4 mM sodium lactate to enhance the purity of the differentiated CMs. After the glucose starvation step, the cells were maintained in RPMI + B27 for further use.

**Gold Electrode Surface Treatment Optimization for hiPSC-CMs Culture.** The gold electrodes were gently washed with 70% ethanol and rinsed with DI water before surface treatment. A circular well was made from polydimethylsiloxane (PDMS) with a diameter of 8 mm and depth of ∼8 mm to hold the media for cell culture. The PDMS well was bonded to the electrode substrate by oxidizing the well and substrate with oxygen plasma and was then baked at 80 °C overnight to secure the covalent bonding (Figure 3A.ii). Since this fabrication process was performed on a rigid parylene-coated glass substrate which does not include any electronics, we were able to use oxygen plasma surface treatment to achieve good attachment. The electrodes were sterilized via UV light radiation and rinsed with PBS with 1% PenStrep. Different methods were applied for enhanced attachment of hiPSC-CMs to the gold electrodes. Matrigel and fibronectin (50 $\mu$g/mL) solutions with and without plasma treatment were deposited in the PDMS wells and incubated at 37 °C for 24 h before cell culture. The extra Matrigel or fibronectin solution was then aspirated from the wells, and a 400 uL cell suspension containing ∼400k hiPSC-CMs was pipetted into each well and incubated at 37 °C. The media was changed every 24h for up to 4 days. Figure 3A.iii shows the entire setup with the cultured cells mounted on the microscope stage for external pulse stimulation and imaging.

**Data Acquisition and Analysis.** Using Zeiss Axio Observer Z1 microscope and ZenPro software, at least three time-lapse videos were recorded at 10× objective for 15 s from different regions of each electrode upon applying the pulses at 0.5, 1.0, and 2 Hz. Then, the beating signals extracted from the videos were analyzed by a custom-written MATLAB code. Electrical voltage and current signals were recorded using a data acquisition system (USB 6361, National Instrument) connected to a laptop computer. Signal monitoring and recording operation were completed in the NI DAQExpress program.

**Live/Dead Assay.** Live/dead standard kit (Life Technology, USA) was used, according to the kit instructions, before and after external pulse stimulation to assess the impact of applied electrical pulses on the viability of the cultured hiPSC-CMs.

**Immunofluorescence (IF) Staining of Cardiac Marker.** The cultured hiPSC-CMs were stained against the sarcomeric alpha-actinin (cardiac-specific marker). Samples were fixed in 4% paraformaldehyde (PFA) at D4 of culture after the second step of external monophasic stimulation and incubated at room temperature (RT) for 20 min. Then, the cells were washed with PBS-glycine 3× for 10 min of incubation at RT. Cells were permeabilized with 0.1% Triton-X-100 for 40 min at RT afterward. To minimize the nonspecific binding of the antibodies, the samples were blocked in 10% goat serum solution for 1 h at RT. The primary cardiac-specific antibody, sarcomeric alpha-actinin, was diluted in the 10% goat serum block solution (1:100). The samples were incubated with the primary antibody solution at 4 °C overnight followed by 5× washing with PBS-tween-20 for 10 min each at RT. Then, the secondary antibody (1:400) was diluted in the 4′,6-diamidino-1-phenylindole (DAPI) (1:1000) solution, centrifuged at 14k RPM for 10 min, and added to the samples for 1 h at RT. Finally, the samples were washed 5× with PBS-tween-20 for 10 min each at RT. Imaging was performed using fluorescence microscopy (Zeiss Axio Observer Z1 with the Zen Pro software suite) equipped with Apotome2 at 20× objective. All the *z*-stack images were reconstructed using the ImageJ software.

**Statistical Analysis.** GraphPad Prism 6 was used to perform the statistical analysis; particularly one-way Anova, to show the statistical differences among the conditions. *P*-value < 0.05 was considered statistically significant for all statistical tests, and error bars represent the mean ± standard deviation (SD).

## RESULTS

**Characterization of the Wireless Stimulator.** Before the wireless stimulator was tested with hiPSC-CMs, we characterized its output voltage and current as a function of transmitted power and distance in open-circuit and cell culture media configurations. The stimulator's output voltage in an open-circuit condition is shown in Figure 2A and B. The output

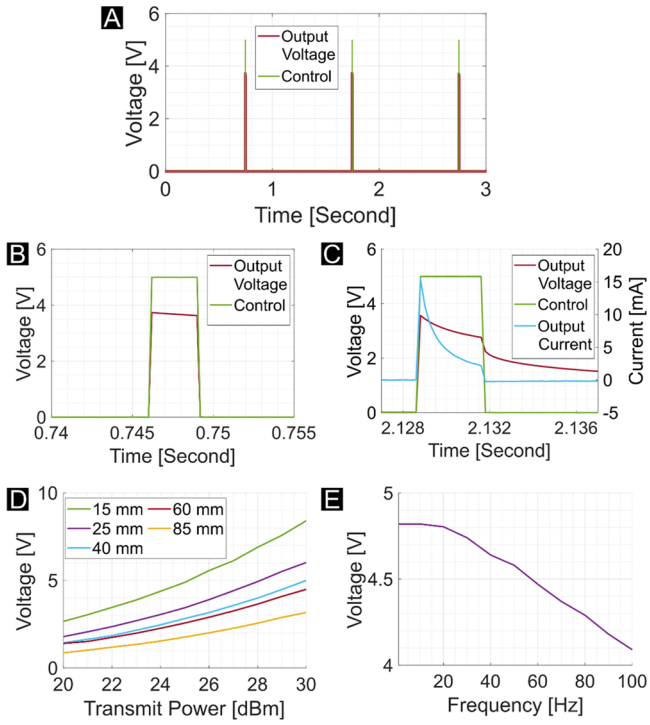


**Figure 2.** Characterization of the proposed wireless stimulator in air ($\varepsilon_r \approx 1$). (A) Stimulator's output voltage as a function of the control signal for a stimulation frequency of 1 Hz. (B) A magnified view showing the pulse width. (C) The stimulator's output voltage and current in cell culturing media. The control signal is inputted to the external transmitter to modulate the RF power transmission; therefore, it directly controls the onset of the stimulation. (D) Magnitude of the output voltage as a function of the transmitted power for several distances between the transmitter and stimulator. (E) Magnitude of the output voltage as a function of the stimulation frequency.

voltage was measured using coated wires (791400, A-M Systems) which were connected to the stimulator output using conductive silver epoxy (12642-14, Electron Microscopy Sciences). The stimulation current passing through cell culture media was found by measuring the voltage across a series sensing resistor with a value of 10 Ohms. The results showed that the stimulator responded to interruptions in the external transmitter's output. A pulse is generated when the external transmitter is switched from a HIGH to a LOW state, where HIGH indicates that a signal is transmitted, and LOW indicates that no signal is transmitted. Figure 2C shows the stimulator's output voltage and current in the presence of cell culture media which can be represented by a resistor in parallel with a constant phase element (CPE).[43] Therefore, the stimulator exhibits a discharging behavior when performing stimulation in the cell culture media. The voltage and current in the cell culture media have a similar waveform, and the measured peak current is around 15.4 mA at a peak voltage of 3.56 V. Figure S-4 includes bode plots of electric impedance spectroscopy (EIS) measurements taken between 1 Hz to 1 MHz at 100 mV. The plots show a large capacitive impedance at low frequency which confirms the measured voltage and current waveforms in Figure 2C.


https://doi.org/10.1021/acssensors.2c00794
ACS Sens. 2022, 7, 3287−3297

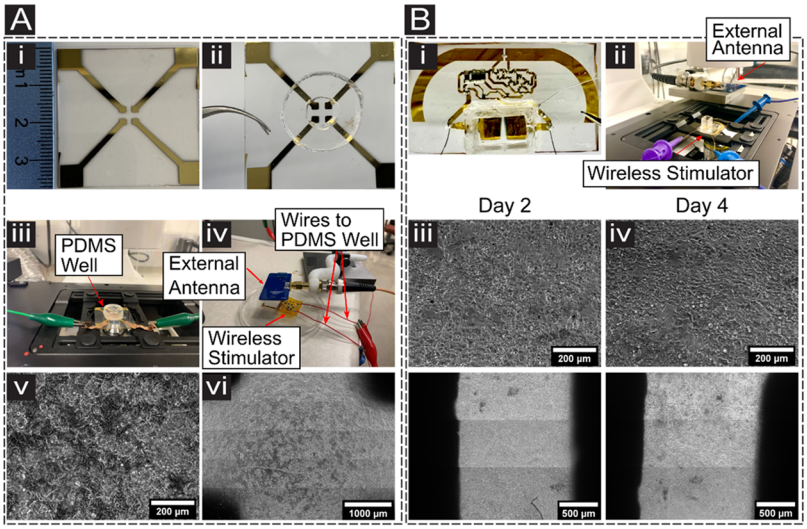


**Figure 3.** (A) (i) Image exhibiting the designed gold electrodes on parylene-coated glass slides that are used for excitability assessment. (ii) The electrodes with the PDMS well adhered through surface plasma treatment. (iii) Image showing the electrodes with the PDMS well mounted on the microscope stage. (iv) Setup of the external antenna and the wireless stimulator fabricated on polyimide.[21] Cables are used to connect the stimulator with the electrodes. (v) Phase-contrast images of the cultured hiPSC-CMs on Matrigel-coated electrodes captured by 10× objective (scale bar: 200 $\mu$m). (vi) The tile-image of hiPSC-CMs on the same surface (scale bar:1000 $\mu$m) on day 2 of culture. (B) (i) Image showing the proposed wireless stimulator fabricated on a parylene/PDMS substrate. (ii) Image of the proposed wireless stimulator and the external antenna placed on the microscope. The wires are connected only for testing purposes. (iii and iv) Phase-contrast images of the cultured hiPSC-CMs on Matrigel-coated electrodes after the first (iii) and second (iv) round of stimulation at days 2 and 4, respectively. (scale bars: 200 (top row) and 500 $\mu$m (bottom row)).

The output voltage of the stimulator circuit was measured at varying transmitted power levels and different distances between the external transmitter and the stimulator circuit, as shown in Figure 2D. The maximum accumulated voltage increased with the transmitted power and decreased with the distance. The maximum measured voltage was 8.4 V at a transmit power of 30 dBm and distance of 15 mm. Note that the output voltage still reached 2 V even when distance was as large as 85 mm. The results shown in Figure 2D demonstrate that the stimulator can operate at a wide range of distances and transmit power values. The maximum accumulated voltage was also a function of the stimulation frequency as shown in Figure 2E. The storage capacitor was fully charged at low stimulation frequencies, but the stored voltage decreased as the stimulation frequency increased beyond 20 Hz. Figure 2E shows that there is adequate time to charge the capacitor when the stimulation frequency is below 20 Hz, which is the range of stimulation frequencies that is needed in most applications.

**Surface Preparation and Optimization for Enhanced Attachment and Culture of hiPSC-CMs.** The proposed wireless stimulator employed gold electrodes fabricated on a thin layer of Parylene that was attached to the PDMS substrate. A key step was to treat the Parylene to enhance the hiPSC-CMs attachment and survival before testing the stimulation of hiPSC-CMs using the proposed wireless stimulator (Figure 3A). Fibronectin and Matrigel have been widely used to coat tissue culture plastics that are intended for hiPSC-CMs culturing.[40,44] Thus, in this work, fibronectin and Matrigel were primarily considered along with plasma treatment to optimize the surface treatment for culturing hiPSC-CMs. Plasma treatment was specifically performed on the electrode surfaces to generate a hydrophilic surface before depositing the fibronectin and Matrigel solutions. As shown in Figure S-5A, cells cultured on Matrigel and Plasma-Matrigel had better distribution and formation of cellular monolayer at day 2 of culture. However, cells cultured on fibronectin and plasma-fibronectin-coated wells did not spread and instead formed cellular aggregates. As part of this optimization, external electrical stimulation was applied to hiPSC-CMs cultured on Matrigel-, plasma-Matrigel-, fibronectin-, and plasma-fibronectin-coated electrodes at day 2. Figure S-5B shows the beating signals extracted from the videos. Stimulation at 0.5 Hz caused irregular beating in all experimental groups; however, at 1.0 and 2.0 Hz, cells cultured on Matrigel-coated electrodes had synchronous beating signals. Based on the preliminary experimental and optimization results, Matrigel coating was selected for the Parylene surface treatment before the culture of hiPSC-CMs for all subsequent experiments.

**Excitability Assessment of the Cultured hiPSC-CMs.** The excitability of the hiPSC-CMs was assessed using a setup composed of a PDMS well that was attached to the gold electrodes sputtered on parylene-coated glass slides as shown in Figure 3**A.i-iv**. Electrical stimulation was delivered to the cells cultured in the PDMS well using the wireless passive stimulator that we designed, fabricated, and tested on a Polyimide substrate[21] (Figure 3A). In this experiment, the voltage pulses generated by the wireless stimulator were delivered to the PDMS well through cables connected between the stimulator and the electrodes inside the PDMS well. An external transmitter, composed of a frequency synthesizer and an antenna was positioned above the stimulator as shown in Figure 3A.iv. hiPSC-CMs cultured on the Matrigel-coated electrodes were well-distributed and presented spontaneous beating after 48 h of culture as shown in Figure 3A.v and vi. On the other hand, Figure 4A shows the beating signals extracted from the recorded videos (top row) upon the stimulation of hiPSC-CMs at 0.5, 1.0, and 2.0 Hz. Compared to 0.5 and 2.0 Hz, cells showed more regular and synchronous beating at 1.0 Hz. The beating frequencies (beats per minute) extracted from three biological replicates were increased as a function of the stimulation frequency as shown in Figure 4B.i. The statistical analysis confirmed that the beating frequency was significantly higher at 2.0 Hz than in other experimental groups. Furthermore, the


https://doi.org/10.1021/acssensors.2c00794
ACS Sens. 2022, 7, 3287−3297

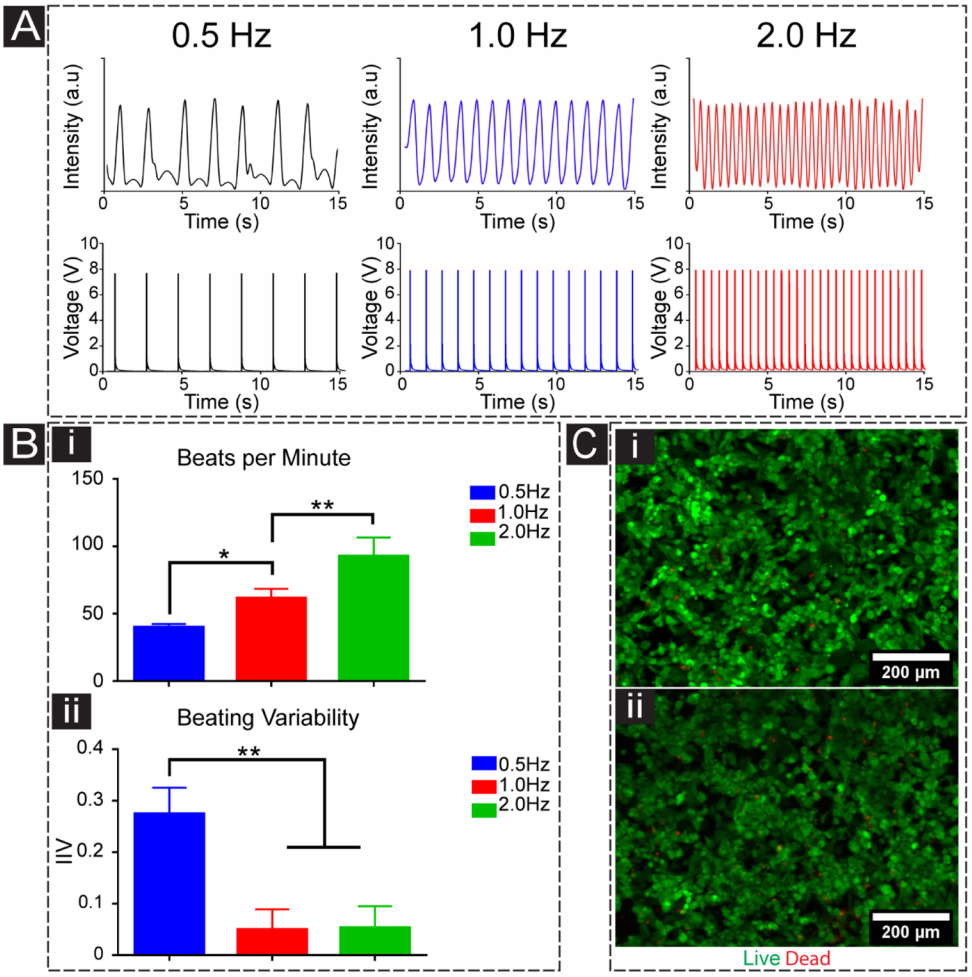


**Figure 4.** Excitability assessment of hiPSC-CMs cultured on electrodes using the wireless stimulator fabricated on polyimide.[21] (A) Beating signals of cells extracted from the recorded videos (top row) under stimulation frequencies of 0.5, 1.0, and 2.0 Hz. The bottom row shows the monophasic stimulation signals that are generated by the stimulator and delivered to hiPSC-CMs. (B) Quantification of beating numbers (beats per minute) (i) and interbeat interval variability (IIV) (ii) ($N = 3$) (*$P < 0.05$, **$P < 0.01$). Error bars represent standard deviation. (C) Fluorescence images showing live (green) and dead (red) dead cells before (i) and after external electrical pulse stimulation (ii) (scale bar: 200 $\mu$m).

peaks of these signals were also extracted to quantify the interbeat interval variability (IIV), considered a quantitative measure of contraction synchronicity. The cells exhibited significantly lower IIV at 1.0 and 2.0 Hz than 0.5 Hz, suggesting that the cells were synchronously beating at 1.0 and 2.0 Hz frequencies as shown in Figure 4B.ii. Live/dead assay was further performed before and after stimulation to confirm that the external pulse stimulation did not negatively affect the viability of the cultured hiPSC-CMs. The fluorescence images showed that cell viability was not significantly different before and after stimulation Figure 4C. Overall, it was demonstrated that the cultured hiPSC-CMs responded to the external stimulation at various frequencies, and the stimulation process did not impact the cell viability.

**Electrical Stimulation of Cultured hiPSC-CMs Using the Proposed Wireless Stimulator.** After assessing the excitability and viability of the cells cultured on parylene, the proposed wireless stimulator was tested by directly culturing and stimulating the hiPSC-CMs in the PDMS well integrated with the stimulator as shown in Figure 3B.i. Wireless stimulation was performed by positioning the external transmitting antenna above the proposed stimulator. Both the external antenna and the stimulator were placed on the microscope stage, as shown in Figure 3B.ii. Owing to the transparency of the stimulator, real-time observation of cell activity was possible during the stimulation process. In this setup, hiPSC-CM stimulation at two different time points (days 2 and 4) was performed to confirm the functionality of the devices after multiple rounds of wireless stimulation. Figure 3B.iii and iv shows the distribution of cells across the surface of the electrodes after the first and second round of wireless stimulation, respectively. The phase-contrast images confirmed that the cells remained viable and adhered to the surface after two rounds of stimulation (days 2 and 4). Similar to the previous setup, wireless stimulation was applied to hiPSC-CMs at 0.5, 1.0, and 2.0 Hz, and videos were recorded for analysis. The external antenna was placed 40 mm from the wireless stimulator, which is within the midfield region of the antenna. At both time points (days 2 and 4), cells responded to the applied pulses and faster beating frequencies were observed as the pulse stimulation was increased (Figure 5A, top row). The top row exhibits the cell beating intensity in arbitrary units in response to the monophasic voltage stimulation pulses that are generated by the stimulator and shown in the bottom row of Figure 5A. The statistical analysis confirmed that the beating frequency (beats per minute) was significantly higher at 2.0 Hz than 0.5 and 1.0 Hz at the two


https://doi.org/10.1021/acssensors.2c00794
ACS Sens. 2022, 7, 3287−3297

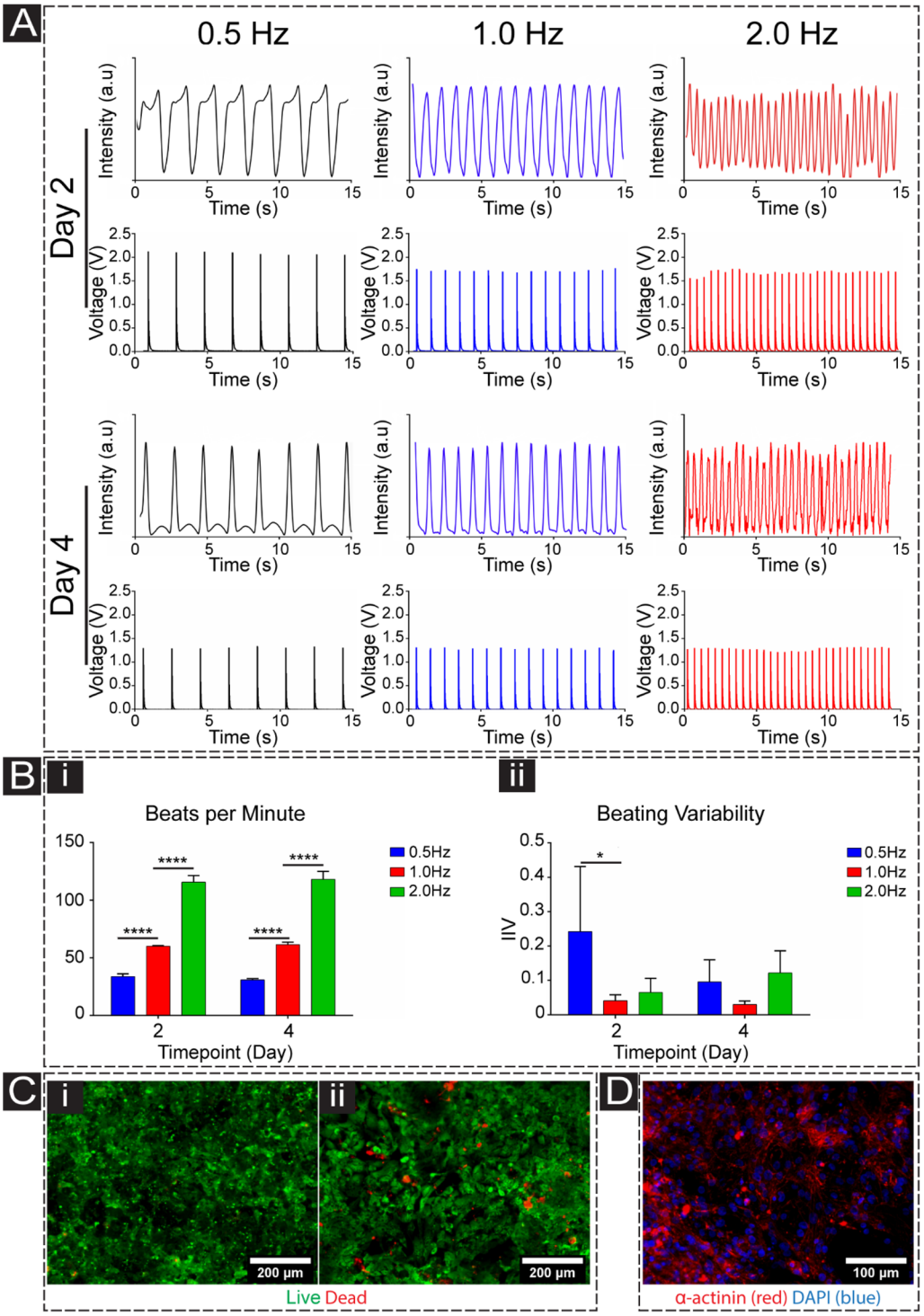


**Figure 5.** Excitability of hiPSC-CMs cultured on the gold electrodes of the proposed wireless stimulator. (A) Beating signals of cells extracted from the recorded videos (top row at each time point) under 0.5, 1.0, and 2.0 Hz stimulation at days 2 and 4 of culture. The bottom row of the data at Day 2 and 4 shows the voltage monophasic stimulation signal that is delivered to the hiPSC-CMs. (B) Quantification of beating numbers (beats per minute) (i) and interbeat interval variability (IIV) (ii) at days 2 and 4 of culture. ($N = 3$) (*$P < 0.05$, ****$P < 0.0001$). Error bars represent standard deviation. (C) Fluorescence images showing live (green) and dead (red) cells after stimulation at days 2 (i) and 4 (ii) of culture (scale bar: 200 $\mu$m). (D) IF image of the sarcomeric alpha-actinin (red) structure of the hiPSC-CMs cultured on Matrigel-coated electrodes after the second round of external stimulation at day 4 (scale bar: 100 $\mu$m).

stimulation time points as shown in Figure 5B.i, suggesting that the proposed wireless stimulator can effectively induce the desired beating frequency of the cultured hiPSC-CMs. Furthermore, at day 2 and 4 of pulse stimulation, lower IIV at 1.0 Hz confirmed the more synchronous beating cells compared to stimulation at 0.5 and 2.0 Hz, as shown in Figure 5B.ii. However, this difference was not significant at day 4 of culture and could be explained by the extended culture time and enhanced maturation of the cultured hiPSC-CMs that caused the cells to respond better to the pulse stimulations.



https://doi.org/10.1021/acssensors.2c00794
ACS Sens. 2022, 7, 3287−3297

**Table I. State-of-the-Art Comparison**

| ref | link/medium | substrate dielectric/$\varepsilon_r$ | freq. GHz | output voltage (V) | distance (mm) | max. Tx power (dBm) | tech. | Rx size (mm$^3$) | Tx size (mm$^2$) |
|---|---|---|---|---|---|---|---|---|---|
| this work[b] | RF/air | parylene PDMS[d]/3 | 2.35 | 8 | 15 | 30 | discrete | 6.9 × 16.7 × 0.6<br>38 × 13 × 0.6[a] | 10 × 10 |
| 25[b] | RF/in-vivo | Rogers TMM/9.8 | 1.2 | <1.8 | 25 | 10 | discrete | 10 × 10 × 1.52 | 230 × 140 |
| 22[c] | RF/in-vivo | soft elastomer | 2.4 | 1 | 10 | 22.6 | discrete | 15 × 3 (diameter) | 27.5 (diameter) |
| 17[c] | coil/in-vivo | FR4/4.2 | 1.3 | <1.5 | 5 | 36 | CMOS | 0.2 × 0.2 × 1.6 | 10 (diameter) |
| 15[c] | coil/in-vivo | polyester | 2.4 | 3 | 15 | 20.49 | discrete | 22 × 23 × 7 | 59 × 88 |

[a]Rectifier size, antenna size, respectively. [b]Cardiac stimulation. [c]Nerve stimulation. [d]Only design with a fully transparent substrate.

A live/dead assay test was performed after each round of stimulation at days 2 and 4 to assess the viability of the cultured hiPSC-CMs. Although some dead cells were observed after stimulation on day 4 as shown in Figure 5C.ii, it was not notably different from day 2 as shown in Figure 5C.i, suggesting that multiple rounds of stimulation did not negatively impact the cell survival and attachment. After the final round of stimulation, multiple samples were fixed and stained against cardiac-specific marker, namely, sarcomeric alpha-actinin, to observe the sarcomere structures of the hiPSC-CMs after external stimulation. The IF images exhibited the striated structure of the hiPSC-CMs cultured on electrodes as seen in Figure 5D. These results confirmed that multiple rounds of electrical pulse stimulation by our proposed wireless stimulator did not negatively affect the cell viability and the phenotype of hiPSC-CMs.

## DISCUSSION

This study reported the design and fabrication of a wireless, battery-free stimulator for the stimulation and pacing of the cultured hiPSC-CMs. The proposed stimulator demonstrates the feasibility for using PDMS as the main substrate for the RF-coupled stimulator, which is engineered by integrating a planar antenna and a Dickson voltage multiplier. The proposed stimulator generates the required monophasic pulse with a high voltage amplitude for cardiac stimulation without any active biasing source, amplification, or complex digital processing. The desired stimulation voltage can be obtained from a simple external transmitter that is composed of an RF signal source and a compact external antenna. The stimulator does not include a voltage regulator because the purpose of this work is to evaluate the stimulator's performance for harvesting RF energy at various distances and transmit power levels. For stimulation of cells, voltage regulation is not needed because we are able to deliver monophasic voltage pulses with a stable amplitude by fixing the distance, transmit power, and stimulation frequency. For future *in vivo* testing, it is possible to include a boost-buck converter or power management unit (PMU) between the rectifier and the storage capacitor to achieve voltage regulation while adopting the same OOK modulation method to control the delivery of stimulation pulses. The cultured hiPSC-CMs were stimulated at various frequencies and remained functional after multirounds of stimulations. Electrical stimulation of engineered heart tissues has been reported in multiple studies through wired equipment.[7−10] Owing to the recently developed electroconductive hydrogels,[45−47] extended electrical stimulation of cardiac tissues could be facilitated by coupling the proposed stimulator with electroconductive hydrogels for the enhanced maturation of cardiac tissues derived from hiPSC-CMs in a 3D environment. The successful excitation of the cardiac cells can provide us with valuable insights for designing the future in vivo version of the wireless stimulator, helping us to minimize the number of required animal experiment trials to obtain successful in vivo results. The proposed wireless stimulation system could also have potential applications in *in vitro* cardiac disease models such as pacing induced heart failure and atrial fibrillation caused by rapid heart rates.[48,49]

In addition to *in vitro* application of this device, the proposed wireless stimulator could be further optimized as a cardiac pacemaker for *in vivo* applications owing to its advantages over other current pacemakers. For *in vivo* applications, the antenna size can be further miniaturized due to the high dielectric constant of the surrounding tissue after implantation.[50] A thin PDMS superstrate may be added to protect the discrete components on the surface. A full electromagnetic simulation of the antenna in a phantom and *in vitro* testing using a liquid or a solid phantom, which mimics the electrical properties of the tissue, can aid in future development of an *in vitro* wireless stimulator.

Table I shows a comparison of the proposed wireless stimulator with similar designs from the literature. Comparing to other work the stimulator proposed in this work exhibit a larger overall size. Note that the size of a stimulator is mainly determined by the largest component, which is usually the antenna (or coil). Reducing the size of the antenna is governed by three constraints: (1) the relative dielectric constant of the surrounding dielectric material; (2) the relative dielectric constant and the thickness of the dielectric substrate on which the antenna is designed and fabricated; and (3) the operating frequency. A higher dielectric constant or operating frequency leads to a smaller antenna. Since the main aim of this work is to test the functionality of the wireless stimulator with cultured hiPSC-CMS, the antenna was designed to operate in air. Compared to other dielectric materials, air has the lowest relative dielectric constant ($\varepsilon_r \approx 1$) which makes it difficult to reduce the size of the antenna. In addition, the proposed wireless stimulator is fabricated on a parylene/PDMS substrate which has the lowest relative dielectric constant and the smallest thickness when compared to other designs in the table, which complicates the task of reducing the antenna size. Nevertheless, this work demonstrated that it is possible to design and fabricate a printed antenna on a parylene/PDMS substrate and use meandering to shrink its size. The size of our stimulator can be further reduced for in vivo application because tissues generally have significantly higher dielectric constants. For example, human muscle and fat tissue have relative dielectric constants of 52.7 and 5.3 at 2.4 GHz, respectively.[51] The reduction in size can be achieved without impacting the main principal of circuit operation. Also, in terms of fabrication method, this work presented a simple, low-cost, and reliable fabrication method where off-the-shelf electronic components can be soldered


https://doi.org/10.1021/acssensors.2c00794
ACS Sens. 2022, 7, 3287−3297

directly on the substrate. In contrast, CMOS fabrication[17] allows designers to shrink the size of the electronics and achieve the smallest size, as shown in Table I, at the expense of increased cost and complexity.

When comparing the output voltage, the proposed wireless stimulator achieves a higher output voltage than all other stimulators operating at same-order frequencies. However, it is important to note that this is achieved in air. We did not use any tissue-emulating phantom to encapsulate the stimulator as this will prohibit us to observe the cell contraction activity. In our future work, we will use a phantom to encapsulate the stimulator device to better mimic the implantation environment, and we expect to see a much lower output voltage value due to the significant RF power loss inside the tissue. However, this drop of output voltage can be compensated by further optimizing our circuit structure. The low stimulation frequency (<2 Hz) enables us to utilize the time interval between each stimulation pulses to accumulate charges, achieving efficient output stimulation voltage even under limited RF power. This can be accomplished by improving our rectifier or adding a low power passive power management unit (PMU). Moreover, to the best of our knowledge, this work is the first to present a passive RF powered stimulator that is fabricated on a Parylene/PDMS substrate. Before this work, PDMS was mainly considered as a coating material but not as the dielectric substrate for wireless stimulator applications.[13,14,34,35] In addition, the proposed wireless stimulator is powered from the smallest external antenna size (tied with the coil in the study in ref 17), and it is the only stimulator fabricated on a biocompatible and transparent substrate.

## CONCLUSION

This paper demonstrated the synchronous cell contraction of hiPSC-CMs in response to external stimulation carried out by a wireless, passive, and biocompatible stimulator fabricated on a flexible and transparent parylene/PDMS substrate. A meandered printed dipole with a gain of 2.2 dBi extends the range of proposed stimulator to 85 mm when tested in air. The stimulator features a simple structure and can deliver a voltage pulse with an amplitude of 8 V at 15 mm distance between the transmitter and stimulator without requiring active circuits to boost the signal. The experimental results showed that the cultured hiPSC-CMs responded well to electrical stimulation at various frequencies. The live/dead assay demonstrated that the cells remained viable after stimulation. Furthermore, the IF stained imaging of the sarcomeric alpha-actinin confirmed that the cellular phenotype of the stimulated hiPSC-CMs was unchanged. These results suggest that the proposed stimulator has a promising potential in the field of tissue engineering and cardiac stimulation. Further miniaturization can be performed in the future to optimize the stimulator for implantable applications.

## ASSOCIATED CONTENT

### Supporting Information

The Supporting Information is available free of charge at https://pubs.acs.org/doi/10.1021/acssensors.2c00794.

Meandered dipole design, detailed fabrication steps, fabrication on a Rogers 6010 Substrate, electric impedance spectroscopy (EIS) measurements, and surface preparation (PDF)

Day 2 contraction of hiPSC-CMs at 0.5, 1.0, and 2.0 Hz (MP4)

Day 4 contraction of hiPSC-CMs at 0.5, 1.0, and 2.0 Hz (MP4)

## AUTHOR INFORMATION


### Corresponding Authors

**Mehdi Nikkhah** − *School of Biological and Health Systems Engineering, Arizona State University, Tempe, Arizona 85281, United States; Center for Personalized Diagnostics (CPD), Biodesign Institute, Arizona State University, Tempe, Arizona 85287, United States*; Email: Mehdi.Nikkhah@asu.edu

**Jennifer Blain Christen** − *School of Electrical, Computer and Energy Engineering, Arizona State University, Tempe, Arizona 85287-5706, United States*; orcid.org/0000-0002-4980-5577; Email: Jennifer.Blainchristen@asu.edu

### Authors

**Ahmed Abed Benbuk** − *School of Electrical, Computer and Energy Engineering, Arizona State University, Tempe, Arizona 85287-5706, United States*; orcid.org/0000-0001-9234-983X

**Hamid Esmaeili** − *School of Biological and Health Systems Engineering, Arizona State University, Tempe, Arizona 85281, United States*

**Shiyi Liu** − *School of Electrical, Computer and Energy Engineering, Arizona State University, Tempe, Arizona 85287-5706, United States*; orcid.org/0000-0002-5653-4955

**Alejandra Patino-Guerrero** − *School of Biological and Health Systems Engineering, Arizona State University, Tempe, Arizona 85281, United States*

**Raymond Q. Migrino** − *Phoenix Veterans Affairs Health Care System, Phoenix, Arizona 85022, United States; University of Arizona College of Medicine, Phoenix, Arizona 85004, United States*

[†]**Junseok Chae** − *School of Electrical, Computer and Energy Engineering, Arizona State University, Tempe, Arizona 85287-5706, United States*

Complete contact information is available at: https://pubs.acs.org/10.1021/acssensors.2c00794

### Author Contributions

[‡]These authors contributed equally to this work.


### Notes

The authors declare no competing financial interest.

[†]Deceased March 25, 2020.

## ACKNOWLEDGMENTS

Research reported in this publication was supported by HHS-NIH: National Institute of Biomedical Imaging and Bioengineering (NIBIB) of the National Institutes of Health under award number R21 EB028396. The authors would like to acknowledge Prof. Junseok Chae as we sadly continue this work without him.

## REFERENCES

(1) Bhatia, N.; El-Chami, M. Leadless Pacemakers: A Contemporary Review. *J. Geriatr. Cardiol. JGC* **2018**, *15* (4), 249−253.

(2) Kirkfeldt, R. E.; Johansen, J. B.; Nohr, E. A.; Jorgensen, O. D.; Nielsen, J. C. Complications after Cardiac Implantable Electronic Device Implantations: An Analysis of a Complete, Nationwide Cohort in Denmark. *Eur. Heart J.* **2014**, *35* (18), 1186−1194.

(3) Udo, E. O.; Zuithoff, N. P. A.; van Hemel, N. M.; de Cock, C. C.; Hendriks, T.; Doevendans, P. A.; Moons, K. G. M. Incidence and Predictors of Short- and Long-Term Complications in Pacemaker

Therapy: The FOLLOWPACE Study. *Heart Rhythm* **2012**, *9* (5), 728−735.
(4) Spickler, J. W.; Rasor, N. S.; Kezdi, P.; Misra, S. N.; Robins, K. E.; LeBoeuf, C. Totally Self-Contained Intracardiac Pacemaker. *J. Electrocardiol.* **1970**, *3* (3−4), 325−331.
(5) Magnusson, P.; Liv, P. Living with a Pacemaker: Patient-Reported Outcome of a Pacemaker System. *BMC Cardiovasc. Disord.* **2018**, *18* (1), 110.
(6) Gist, K. M.; Marino, B. S.; Palmer, C.; Fish, F. A.; Moore, J. P.; Czosek, R. J.; Cassedy, A.; LaPage, M. J.; Law, I. H.; Garnreiter, J.; Cannon, B. C.; Collins, K. K. Cosmetic Outcomes and Quality of Life in Children with Cardiac Implantable Electronic Devices. *Pacing Clin. Electrophysiol.* **2019**, *42* (1), 46−57.
(7) Lasher, R. A.; Pahnke, A. Q.; Johnson, J. M.; Sachse, F. B.; Hitchcock, R. W. Electrical Stimulation Directs Engineered Cardiac Tissue to an Age-Matched Native Phenotype. *J. Tissue Eng.* **2012**, *3* (1), 204173141245535.
(8) Hirt, M. N.; Boeddinghaus, J.; Mitchell, A.; Schaaf, S.; Börnchen, C.; Müller, C.; Schulz, H.; Hubner, N.; Stenzig, J.; Stoehr, A.; Neuber, C.; Eder, A.; Luther, P. K.; Hansen, A.; Eschenhagen, T. Functional Improvement and Maturation of Rat and Human Engineered Heart Tissue by Chronic Electrical Stimulation. *J. Mol. Cell. Cardiol.* **2014**, *74*, 151−161.
(9) Ruan, J.-L.; Tulloch, N. L.; Razumova, M. V.; Saiget, M.; Muskheli, V.; Pabon, L.; Reinecke, H.; Regnier, M.; Murry, C. E. Mechanical Stress Conditioning and Electrical Stimulation Promote Contractility and Force Maturation of Induced Pluripotent Stem Cell-Derived Human Cardiac Tissue. *Circulation* **2016**, *134* (20), 1557−1567.
(10) Ronaldson-Bouchard, K.; Ma, S. P.; Yeager, K.; Chen, T.; Song, L.; Sirabella, D.; Morikawa, K.; Teles, D.; Yazawa, M.; Vunjak-Novakovic, G. Advanced Maturation of Human Cardiac Tissue Grown from Pluripotent Stem Cells. *Nature* **2018**, *556* (7700), 239−243.
(11) Veldhuizen, J.; Migrino, R. Q.; Nikkhah, M. Three-Dimensional Microengineered Models of Human Cardiac Diseases. *J. Biol. Eng.* **2019**, *13* (1), 29.
(12) Radisic, M.; Park, H.; Shing, H.; Consi, T.; Schoen, F. J.; Langer, R.; Freed, L. E.; Vunjak-Novakovic, G. Functional Assembly of Engineered Myocardium by Electrical Stimulation of Cardiac Myocytes Cultured on Scaffolds. *Proc. Natl. Acad. Sci. U. S. A.* **2004**, *101* (52), 18129−18134.
(13) Gutruf, P.; Yin, R. T.; Lee, K. B.; Ausra, J.; Brennan, J. A.; Qiao, Y.; Xie, Z.; Peralta, R.; Talarico, O.; Murillo, A.; Chen, S. W.; Leshock, J. P.; Haney, C. R.; Waters, E. A.; Zhang, C.; Luan, H.; Huang, Y.; Trachiotis, G.; Efimov, I. R.; Rogers, J. A. Wireless, Battery-Free, Fully Implantable Multimodal and Multisite Pacemakers for Applications in Small Animal Models. *Nat. Commun.* **2019**, *10* (1), 5742.
(14) Choi, Y. S.; Yin, R. T.; Pfenniger, A.; Koo, J.; Avila, R.; Benjamin Lee, K.; Chen, S. W.; Lee, G.; Li, G.; Qiao, Y.; Murillo-Berlioz, A.; Kiss, A.; Han, S.; Lee, S. M.; Li, C.; Xie, Z.; Chen, Y.-Y.; Burrell, A.; Geist, B.; Jeong, H.; Kim, J.; Yoon, H.-J.; Banks, A.; Kang, S.-K.; Zhang, Z. J.; Haney, C. R.; Sahakian, A. V.; Johnson, D.; Efimova, T.; Huang, Y.; Trachiotis, G. D.; Knight, B. P.; Arora, R. K.; Efimov, I. R.; Rogers, J. A. Fully Implantable and Bioresorbable Cardiac Pacemakers without Leads or Batteries. *Nat. Biotechnol.* **2021**, *39* (10), 1228−1238.
(15) Xu, Q.; Hu, D.; Duan, B.; He, J. A Fully Implantable Stimulator With Wireless Power and Data Transmission for Experimental Investigation of Epidural Spinal Cord Stimulation. *IEEE Trans. Neural Syst. Rehabil. Eng.* **2015**, *23* (4), 683−692.
(16) Yeh, K.-Y.; Chiu, H.-W.; Tseng, W.-T.; Chen, H.-C.; Yen, C.-T.; Lu, S.-S.; Lin, M.-L. A Dual-Mode Multifunctional Pulsed Radio-Frequency Stimulator for Trigeminal Neuralgia Relief and Its Animal Model. *IEEE Trans. Biomed. Circuits Syst.* **2021**, *15* (4), 719−730.
(17) Khalifa, A.; Karimi, Y.; Wang, Q.; Montlouis, W.; Garikapati, S.; Stanacevic, M.; Thakor, N.; Etienne-Cummings, R. The Microbead: A Highly Miniaturized Wirelessly Powered Implantable Neural Stimulating System. *IEEE Trans. Biomed. Circuits Syst.* **2018**, *12* (3), 521−531.
(18) Lyu, H.; Wang, J.; La, J.-H.; Chung, J. M.; Babakhani, A. An Energy-Efficient Wirelessly Powered Millimeter-Scale Neurostimulator Implant Based on Systematic Codesign of an Inductive Loop Antenna and a Custom Rectifier. *IEEE Trans. Biomed. Circuits Syst.* **2018**, *12* (5), 1131−1143.
(19) Iqbal, A.; Al-Hasan, M.; Mabrouk, I. B.; Basir, A.; Nedil, M.; Yoo, H. Biotelemetry and Wireless Powering of Biomedical Implants Using a Rectifier Integrated Self-Diplexing Implantable Antenna. *IEEE Trans. Microw. Theory Technol.* **2021**, *69* (7), 3438−3451.
(20) Basir, A.; Yoo, H. Efficient Wireless Power Transfer System With a Miniaturized Quad-Band Implantable Antenna for Deep-Body Multitasking Implants. *IEEE Trans. Microw. Theory Technol.* **2020**, *68* (5), 1943−1953.
(21) Liu, S.; Navaei, A.; Meng, X.; Nikkhah, M.; Chae, J. Wireless Passive Stimulation of Engineered Cardiac Tissues. *ACS Sens.* **2017**, *2* (7), 1006−1012.
(22) Tanabe, Y.; Ho, J. S.; Liu, J.; Liao, S.-Y.; Zhen, Z.; Hsu, S.; Shuto, C.; Zhu, Z.-Y.; Ma, A.; Vassos, C.; Chen, P.; Tse, H. F.; Poon, A. S. Y. High-Performance Wireless Powering for Peripheral Nerve Neuromodulation Systems. *PLoS One* **2017**, *12* (10), e0186698.
(23) Bakogianni, S.; Koulouridis, S. A Dual-Band Implantable Rectenna for Wireless Data and Power Support at Sub-GHz Region. *IEEE Trans. Antennas Propag.* **2019**, *67* (11), 6800−6810.
(24) Ding, S.; Koulouridis, S.; Pichon, L. Implantable Wireless Transmission Rectenna System for Biomedical Wireless Applications. *IEEE Access* **2020**, *8*, 195551−195558.
(25) Asif, S. M.; Hansen, J.; Khan, M. S.; Walden, S. D.; Jensen, M. O.; Braaten, B. D.; Ewert, D. L. Design and In Vivo Test of a Batteryless and Fully Wireless Implantable Asynchronous Pacing System. *IEEE Trans. Biomed. Eng.* **2016**, *63* (5), 1070−1081.
(26) Zada, M.; Yoo, H. A Miniaturized Triple-Band Implantable Antenna System for Bio-Telemetry Applications. *IEEE Trans. Antennas Propag.* **2018**, *66* (12), 7378−7382.
(27) Yang, Z.-J.; Xiao, S.-Q.; Zhu, L.; Wang, B.-Z.; Tu, H.-L. A Circularly Polarized Implantable Antenna for 2.4-GHz ISM Band Biomedical Applications. *IEEE Antennas Wirel. Propag. Lett.* **2017**, *16*, 2554−2557.
(28) Abbas, S. M.; Desai, S. C.; Esselle, K. P.; Volakis, J. L.; Hashmi, R. M. Design and Characterization of a Flexible Wideband Antenna Using Polydimethylsiloxane Composite Substrate. *Int. J. Antennas Propag.* **2018**, *2018*, 1−6.
(29) Kim, S.; Towfeeq, I.; Dong, Y.; Gorman, S.; Rao, A.; Koley, G. P(VDF-TrFE) Film on PDMS Substrate for Energy Harvesting Applications. *Appl. Sci.* **2018**, *8* (2), 213.
(30) Simorangkir, R. B. V. B.; Yang, Y.; Matekovits, L.; Esselle, K. P. Dual-Band Dual-Mode Textile Antenna on PDMS Substrate for Body-Centric Communications. *IEEE Antennas Wirel. Propag. Lett.* **2017**, *16*, 677−680.
(31) Janapala, D. K.; Nesasudha, M.; Mary Neebha, T.; Kumar, R. Design and Development of Flexible PDMS Antenna for UWB-WBAN Applications. *Wirel. Pers. Commun.* **2022**, *122* (4), 3467−3483.
(32) Sharma, P. K.; Gupta, N.; Dankov, P. I. Characterization of Polydimethylsiloxane (PDMS) as a Wearable Antenna Substrate Using Resonance and Planar Structure Methods. *AEU - Int. J. Electron. Commun.* **2020**, *127*, 153455.
(33) Bakar, A. A.; Hasnan, F.; Razali, A. R.; Rahim, A. F. A.; Osman, M. S.; Ali, T.; Radzali, R. Polydimethylsiloxane as a Potential Antenna Substrate. *Acta Phys. Polym., A* **2019**, *135* (5), 938−941.
(34) Charthad, J.; Chang, T. C.; Liu, Z.; Sawaby, A.; Weber, M. J.; Baker, S.; Gore, F.; Felt, S. A.; Arbabian, A. A Mm-Sized Wireless Implantable Device for Electrical Stimulation of Peripheral Nerves. *IEEE Trans. Biomed. Circuits Syst.* **2018**, *12* (2), 257−270.
(35) Lee, B.; Koripalli, M. K.; Jia, Y.; Acosta, J.; Sendi, M. S. E.; Choi, Y.; Ghovanloo, M. An Implantable Peripheral Nerve Recording and Stimulation System for Experiments on Freely Moving Animal Subjects. *Sci. Rep.* **2018**, *8* (1), 6115.
(36) Oyunbaatar, N.-E.; Shanmugasundaram, A.; Jeong, Y.-J.; Lee, B.-K.; Kim, E.-S.; Lee, D.-W. Micro-Patterned SU-8 Cantilever Integrated with Metal Electrode for Enhanced Electromechanical Stimulation of Cardiac Cells. *Colloids Surf. B Biointerfaces* **2020**, *186*, 110682.
(37) Min, S.; Lee, H.-J.; Jin, Y.; Kim, Y. H.; Sung, J.; Choi, H.-J.; Cho, S.-W. Biphasic Electrical Pulse by a Micropillar Electrode Array

Enhances Maturation and Drug Response of Reprogrammed Cardiac Spheroids. *Nano Lett.* **2020**, *20* (10), 6947−6956.
(38) Nunes, S. S.; Miklas, J. W.; Liu, J.; Aschar-Sobbi, R.; Xiao, Y.; Zhang, B.; Jiang, J.; Massé, S.; Gagliardi, M.; Hsieh, A.; Thavandiran, N.; Laflamme, M. A.; Nanthakumar, K.; Gross, G. J.; Backx, P. H.; Keller, G.; Radisic, M. Biowire: A Platform for Maturation of Human Pluripotent Stem Cell−Derived Cardiomyocytes. *Nat. Methods* **2013**, *10* (8), 781−787.
(39) Obeid, D.; Issa, G.; Sadek, S.; Zaharia, G.; El Zein, G. Low Power Microwave Systems for Heartbeat Rate Detection at 2.4, 5.8, 10 and 16 GHz. In *2008 First International Symposium on Applied Sciences on Biomedical and Communication Technologies*; IEEE: Aalborg, Denmark, 2008; pp 1−5. DOI: 10.1109/ISABEL.2008.4712623.
(40) Lian, X.; Zhang, J.; Azarin, S. M.; Zhu, K.; Hazeltine, L. B.; Bao, X.; Hsiao, C.; Kamp, T. J.; Palecek, S. P. Directed Cardiomyocyte Differentiation from Human Pluripotent Stem Cells by Modulating Wnt/$\beta$-Catenin Signaling under Fully Defined Conditions. *Nat. Protoc.* **2013**, *8* (1), 162−175.
(41) Veldhuizen, J.; Cutts, J.; Brafman, D. A.; Migrino, R. Q.; Nikkhah, M. Engineering Anisotropic Human Stem Cell-Derived Three-Dimensional Cardiac Tissue on-a-Chip. *Biomaterials* **2020**, *256*, 120195.
(42) Veldhuizen, J.; Chavan, R.; Moghadas, B.; Park, J. G.; Kodibagkar, V. D.; Migrino, R. Q.; Nikkhah, M. Cardiac Ischemia On-a-Chip to Investigate Cellular and Molecular Response of Myocardial Tissue under Hypoxia. *Biomaterials* **2022**, *281*, 121336.
(43) Brug, G. J.; van den Eeden, A. L. G.; Sluyters-Rehbach, M.; Sluyters, J. H. The Analysis of Electrode Impedances Complicated by the Presence of a Constant Phase Element. *J. Electroanal. Chem. Interfacial Electrochem.* **1984**, *176* (1−2), 275−295.
(44) Herron, T. J.; Rocha, A. M. D.; Campbell, K. F.; Ponce-Balbuena, D.; Willis, B. C.; Guerrero-Serna, G.; Liu, Q.; Klos, M.; Musa, H.; Zarzoso, M.; Bizy, A.; Furness, J.; Anumonwo, J.; Mironov, S.; Jalife, J. Extracellular Matrix−Mediated Maturation of Human Pluripotent Stem Cell−Derived Cardiac Monolayer Structure and Electrophysiological Function. *Circ. Arrhythm. Electrophysiol.* **2016**, DOI: 10.1161/CIRCEP.113.003638.
(45) Esmaeili, H.; Patino-Guerrero, A.; Hasany, M.; Ansari, M. O.; Memic, A.; Dolatshahi-Pirouz, A.; Nikkhah, M. Electroconductive Biomaterials for Cardiac Tissue Engineering. *Acta Biomater.* **2022**, *139*, 118−140.
(46) Navaei, A.; Saini, H.; Christenson, W.; Sullivan, R. T.; Ros, R.; Nikkhah, M. Gold Nanorod-Incorporated Gelatin-Based Conductive Hydrogels for Engineering Cardiac Tissue Constructs. *Acta Biomater.* **2016**, *41*, 133−146.
(47) Patino-Guerrero, A.; Veldhuizen, J.; Zhu, W.; Migrino, R. Q.; Nikkhah, M. Three-Dimensional Scaffold-Free Microtissues Engineered for Cardiac Repair. *J. Mater. Chem. B* **2020**, *8* (34), 7571−7590.
(48) Klocke, R.; Tian, W.; Kuhlmann, M.; Nikol, S. Surgical Animal Models of Heart Failure Related to Coronary Heart Disease. *Cardiovasc. Res.* **2007**, *74* (1), 29−38.
(49) Nishida, K.; Michael, G.; Dobrev, D.; Nattel, S. Animal Models for Atrial Fibrillation: Clinical Insights and Scientific Opportunities. *Europace* **2010**, *12* (2), 160−172.
(50) Blauert, J.; Kang, Y.-S.; Kiourti, A. *In Vivo* Testing of a Miniature 2.4/4.8 GHz Implantable Antenna in Postmortem Human Subject. *IEEE Antennas Wirel. Propag. Lett.* **2018**, *17* (12), 2334−2338.
(51) Vallejo, M.; Recas, J.; del Valle, P.; Ayala, J. Accurate Human Tissue Characterization for Energy-Efficient Wireless On-Body Communications. *Sensors* **2013**, *13* (6), 7546−7569.


https://doi.org/10.1021/acssensors.2c00794
*ACS Sens.* 2022, 7, 3287−3297